

**GROUND TRUTH LOCATIONS USING SYNERGY BETWEEN REMOTE SENSING AND SEISMIC METHODS**

Gene A. Ichinose<sup>1</sup>, Hong Kie Thio<sup>2</sup>, and Don V. Helmberger<sup>3</sup>

AFTAC/TTR/MTC<sup>1</sup>, URS Group Inc.<sup>2</sup>, and California Institute of Technology<sup>3</sup>

Sponsored by National Nuclear Security Administration  
Office of Nonproliferation Research and Development  
Office of Defense Nuclear Nonproliferation

Contract No. DE-AC52-03NA99505/BAA03-72

**ABSTRACT**

In this study, we have relocated a set of 50 ground truth (GT) earthquakes as determined from regional modeling, to estimate the performance of the station correction methodology. We constructed station-specific source correction or “station correction” surface from 760 station corrections (global distribution) based on a small set of five well and closely located earthquakes in the central Tibetan Plateau. The station corrections were interpolated to develop a global surface for P-wave travel time corrections. As a test, we relocated a set of 50 GT earthquakes, with some seismic events located about 800 km from the center of the PASSCAL array across the Tibetan Plateau and surrounding regions. When the corrections were applied to the iasp91 velocity model, the mislocations decreased by an average by 37% for 37 out of the 50 GT events. This indicates significant improvement in seismic event locations relative to using the iasp91 model without P-wave travel-time corrections. Surprisingly, the distribution of mislocations did not vary or correlate with distance and some of the farthest events from the center of the Tibetan Plateau were improved more than the locations in the center where the travel time corrections are more relevant. Myers and Schultz (2000) noted that correction surfaces for nearby stations are similar, suggesting coherent variations between the one-dimensional (1D) velocity model and the true velocity structure. Based on the assessment of the results, corrections could be developed from a small cluster of earthquakes and transported for use with seismic events outside of this area out to a radius of 800 km. Additional tests should be performed to further validate these claims especially when crossing tectonic boundaries. This type of calibration and predicted transportability of the P-wave travel-time station corrections will make it more useful for regions of little to no tectonic activity or areas where detailed three-dimensional (3D) velocity model calibration has not yet been performed because of the ease of use in the application of the station correction methodology.

### **OBJECTIVES**

The development of the International Monitoring System (IMS) is intended to meet the monitoring requirements of the Comprehensive Nuclear-Test-Ban Treaty (CTBT). One requirement is the location of seismic events with an uncertainty of less than 1000 km<sup>2</sup> for earthquakes with a magnitude smaller than 4. This has motivated a number of recent studies to develop methods for improving the accuracy and precision of seismic event locations, especially with sparse datasets. These studies can be divided into two categories: calibration-based and model-based. The focus of the calibration-based method is the determination of station or source specific corrections using 1D velocity models, whereas the focus of the model-based method is the development and use of 3D velocity models. Examples of calibration-based studies include Bondar and North (1999), Yang et al. (2001), Richards-Dinger and Shearer (2000), Myers and Schultz (2000), Thurber et al. (2001), and Trabant and Thurber (2001). The former two studies are also examples of the use of spatially varying path corrections for location calibration over large regions. Examples of model-based studies include Smith and Ekstrom (1996) global-scale 3D model tests, Firtas (2000) regional-scale 3D model tests, and Thurber et al. (2001) local-scale 3D model tests. We note that station corrections, which are constant correction values common to a cluster of seismic events are also often included in 3D model solutions at all scales.

Our focus of this paper is on testing the range of applicability of the calibration-based station correction methodology. The correction uncertainties are greatly dependent on the accuracy of the origin time and hypocentral location of seismic events used both in the calibration stage of the corrections and in the testing stage. Since calibration-based station corrections or station-specific source corrections are constructed from GT events that are rare or often difficult to estimate accurately, then testing for transportability will provide information on its applicability in the location of seismic events in sparsely monitored and seismically inactive regions. This information can also be useful for generally improving the earthquake locations for tectonic interpretations using global earthquake catalogs.

We will reduce the uncertainties in testing the station corrections by using 50 GT earthquakes defined by Bondar and North (1999) with epicenter uncertainties on the order of 5 to 10 km (i.e., GT5 to GT10). Each station can have a P-wave travel time correction for a specific source region and that correction will be applied to other earthquakes expanding out to distance offsets on the order of 100s km. The station corrections can be composed from a single or multiple GT events. We do not use source specific station corrections (SSSC) because the event coverage for any particular station is not well distributed and the focus is to evaluate the correction methodology for a cluster of events with a set of station corrections. When using multiple seismic events, stations that did not record at least two of the seismic events within a cluster are set to zero, a background value or a value that is interpolated between stations.

### **RESEARCH ACOMPLISHED**

All ground truth locations and origin times used in this study are taken from the catalog developed by Zhu et al. (2006). They developed a regional 1D P-wave velocity model starting with the International Seismological Centre (ISC) locations and phase arrival data. Using additional phase arrivals and waveform data from the Sino-U.S. PASSCAL seismic recording experiment on the Tibetan Plateau (Owens et al., 1993), Zhu et al. (2006) computed Green's functions from their calibrated model. They then improved the estimates of the focal mechanisms and source depths using the Cut and Paste (CAP) waveform inversion methodology (e.g., Zhu and Helmberger, 1996) with the calibrated Green's functions. They applied a non-linear approach that does not depend on an initial model, which iteratively and simultaneously estimates the velocity model and relocates the hypocenters. They relocated about 50 seismic events recorded by the PASSCAL array between 1991 and 1992 (e.g., Zhu et al., 2006; Tan et al., 2006). These locations are shown in Figure 1 and all events are located within 7 degrees (~800 km) of the center of the PASSCAL array. Based on the analysis of the waveform data and calibration of velocity model, the locations of these events are likely to be uncertain by about 5 to 10 km, (D. Helmberger, Personal Communication).

We use the iasp91 velocity model as a 1D global reference velocity model commonly used as the default in most operational settings. Since the GT catalog of earthquakes by Zhu et al. (2006) has been calibrated to a unique local Tibetan Plateau velocity model, we therefore remove any shifts or biases in origin times due to the difference between the local and global velocity models. We fix the location latitude, longitude, and depth and redetermine the origin time using the global iasp91 model to remove any bias.

We selected five seismic events located near the center of the PASSCAL array that were well recorded globally. These five events were used to calibrate the P-wave travel-time corrections. They ranged in size from  $M_w$  4.1 to 4.7 with 26 to 96 ISC recording stations. If there were 2 or more P-wave recordings for a station between the five events, the average P-wave residual was used in the P-wave travel-time correction surface; otherwise, it was either set to zero or interpolated from 2 or more nearby stations with more data. The average residual was used in the P-wave travel-time corrections if it was larger than one standard deviation. We assume that the average residual is the correction so that it can be added to the travel time for a particular station in future relocations as a correction term. The station corrections were then gridded to develop a global surface by interpolation between data points. The interpolation was performed using the nearest neighbor algorithm (e.g., Wessel and Smith, 1998). We assume that the P-wave travel-time correction surface goes to zero when no data are present. The grid node interval was set to 1 by 1 degree. A circular area with a 15 km search radius is centered on each node with only 1 sector. The average value is computed as a weighted mean of the nearest point from each sector inside the search radius. The weighting function used is  $w(r) = \frac{1}{1+d^2}$ , where  $d = 3\left(\frac{r}{R}\right)$ ,  $R$  is the search radius and  $r$  is distance from the node.

This weight is modulated by the observation points' weights. We compared the multi-event P-wave travel-time correction surface by comparison with a surface constructed using just one of the largest events (Julian day 222) that was an  $M_w$  4.7 with 92 phase arrivals. The resulting surface was very similar in amplitude but slightly different in fine details within 30 degrees due to the increased number of events used in the multi-event correction surface.

We checked the location, depth, and focal mechanism for 10 of the largest earthquakes in the Zhu et al (2006) GT catalog using the regional, long period full waveform moment tensor inversion method (e.g., Ichinose et al., 2003). We performed an inversion on the PASSCAL data recorded by very broadbanded instruments to estimate the centroid origin time, location, and depth, as well as the 5-degrees-of-freedom moment tensor using an a priori velocity model appropriate for the region. The inversion results suggest that all 10 events had double couple mechanism. The differences in depth and locations were within good agreement and only a few km different. The mechanisms were all similar within 10 degrees in strike, dip, and rake and within 0.1 in scalar moment magnitude. The largest differences in location and origin time were for events that had poor station coverage along the outer edges of the PASSCAL array.

Earthquake locations and residual calculations were performed using a grid search routine that used iasp91 travel time tables calculated for discrete distances and depths optimally selected and commonly used in LocSAT (IDC, 1999). The program TauP (Crotwell et al., 1998) was used to calculate the travel-time tables. The appropriate travel-time table is loaded given a source and receiver distance, source depth, and appropriate phase type. A cubic spline is fit to the table values, and the approximate travel-time value is estimated for the source-receiver pair.

Figure 2 shows the global P-wave travel-time correction surface constructed from 760 station correction estimates ranging from  $-4.0$  to  $+2.5$  seconds with average and median values at approximately zero. The largest negative corrections were distributed in India, Southeast Asia, and Australia, but there were no strong positive corrections mapped for this source region.

We located the 50 earthquakes in the GT catalog (Table 1), first without and then with the corrections and computed the mislocation vectors relative to GT locations. The relocations are performed using the previously described grid search algorithm, and the residuals are not weighted by the distance or residual size typically employed in location programs to improve locations in the presence of poor quality data due to bad picks and high noise. The average mislocation was 19.5 km ( $\pm 1\sigma = 10.4$  km) without the correction and 15.4 ( $\pm 1\sigma = 8.9$  km) with the correction. The median mislocation also decreased to 13.8 km with the correction down from 19.3 km without the correction indicating the distributions of mislocations changed from a Gaussian "normal" distribution to one more skewed toward smaller mislocation distances. Figure 3 shows the improvement in locations after the corrections relative to the uncorrected locations. The larger the symbol, the closer in distance the relocation is to the GT location before using the correction. These improvements in relocations do not show any spatial pattern when corrections are applied to seismic events far outside the original source region used in the correction calibration. They are not correlated with distance from the center of the array. Some of the GT test events were out farther than 5 degrees ( $\sim 500$  km) from the source area where corrections are calculated. The events farthest from the center of the array show the largest improvement in location. Overall, 37 of the 50 earthquakes examined improved by an average of 37% (Figure 4; Table 1). The column in Table 1 showing  $\Gamma$  represents the percent improvement using station corrections (SC) between (1) and (2).

### CONCLUSIONS AND RECOMMENDATIONS

In this study, we have relocated a set of 50 GT earthquakes as determined from regional modeling, to estimate the performance of the station correction methodology. We constructed station-specific source correction or “station correction” surface from 760 station corrections (global distribution) based on a small set of five well and closely located earthquakes in the central Tibetan Plateau. The station corrections were interpolated to develop a global surface for P-wave travel time corrections. As a test, we relocated a set of 50 GT earthquakes, with some seismic events located about 800 km from the center of the PASSCAL array across the Tibetan Plateau and surrounding regions. When the corrections were applied to the iasp91 velocity model, the mislocations decreased by an average by 37% for 37 out of the 50 GT events. This indicates significant improvement in seismic event locations relative to using the iasp91 model without P-wave travel-time corrections. Surprisingly, the distribution of mislocations did not vary or correlate with distance, and some of the farthest events from the center of the Tibetan Plateau were improved more than the locations in the center where the travel time corrections are more relevant. Myers and Schultz (2000) noted that correction surfaces for nearby stations are similar, suggesting coherent variations between the one-dimensional velocity model and the true velocity structure. Based on the assessment of the results, corrections could be developed from a small cluster of earthquakes and transported for use with seismic events outside of this area out to a radius of 800 km. Additional tests should be performed to further validate these claims, especially when crossing tectonic boundaries. This type of calibration and predicted transportability of the P-wave travel-time station corrections will make it more useful for regions of little to no tectonic activity or areas where detailed 3D velocity model calibration has not yet been performed, because of the ease of use in the application of the station correction methodology.

### REFERENCES

- Bondar, I. and R. G. North (1999). Development of calibration techniques for the Comprehensive Nuclear-Test-Ban Treaty (CTBT) international monitoring system, *Phys. Earth Planet. Int.* 113: 11–24.
- Crotwell, H. P., T. J. Owens, and J. Ritsema (1999). The TauP ToolKit: Flexible seismic travel-time and ray-path utilities, *Seism. Res. Lett.* 70: 154–160.
- Ichinose, G. A., J. G. Anderson, K. D. Smith, and Y. Zeng (2003). Source parameters of eastern California and western Nevada earthquakes from regional moment tensor inversion, *Bull. Seism. Soc. Am.* 93: 61–84.
- IDC (1999), IDC processing of seismic, hydroacoustic, and infrasonic data, *IDC Documentation 5.2.1*, 302.
- Myers, S. C. and S. C. Schultz (2000). Improving sparse network seismic location with Bayesian kriging and teleseismically constrained calibration events, *Bull. Seism. Soc. Am.* 90: 199–211.
- Owens, T. J., G. E. Randall, F. T. Wu, and R. S. Zeng (1993). PASSCAL instrument performance during the Tibetan plateau passive seismic experiment, *Bull. Seism. Soc. Am.* 83: 1959–1970.
- Richards-Dinger, K. B. and P. M. Shearer, P.M. (2000). Earthquake locations in southern California obtained using source-specific station terms, *J. Geophys. Res.* 105: 10,930–10,960.
- Smith, G. P. and G. Ekstrom (1996). Improving teleseismic earthquake locations using a three-dimensional Earth model, *Bull. Seism. Soc. Am.* 86: 788–796.
- Thurber, C. H., C. M. Trabant, F. Haslinger, and R. Hartog (2001). Nuclear explosion locations at the Balapan, Kazakhstan, nuclear test site: the effects of high-precision arrival times and three-dimensional structure, *Phys. Earth Planet. Int.* 123: 283–301.
- Trabant, C. and C. Thurber (2001). Ground truth events and location capability at Degelen Mountain, Kazakhstan, *Phys. Earth Planet. Int.* (submitted).
- Tan, Y., L. Zhu, D. V. Helmberger, and C. Saikia (2006). Locating and modeling regional earthquakes with two stations, *J. Geophys. Res.* 111: (B01306), doi:10.1029/2005JB003775.

## 29th Monitoring Research Review: Ground-Based Nuclear Explosion Monitoring Technologies

Wessel, P. and W. H. F. Smith (1998). New improved version of GMT released, *EOS Trans., AGU*, 79: 574.

Zhu, L., Y. Tan, D. V. Helmberger, and C. Saikia (2006). Calibration of the Tibetan Plateau using regional seismic waveforms, *Pageoh* (in press).

Zhu, L. and D. V. Helmberger (1996). Advancement in source estimation techniques using broadband regional seismograms, *Bull. Seism. Soc. Am.* 86: 1634–1641.

**29th Monitoring Research Review: Ground-Based Nuclear Explosion Monitoring Technologies**

**Table 1. The CAP origin times, locations and mislocation vectors calculated from relocations using iasp91 without “station corrections” SC(1), iasp91 with SC(2), and published ISC(3) location.**

ID	Date (y/m/d)	Time (h:m)	Lat	Lon	$\Delta r(1)$ (km)	$\Phi(1)$ (°)	$\Delta r(2)$ (km)	$\Phi(2)$ (°)	$\Delta r(3)$ (km)	$\Phi(3)$ (°)	$\Gamma$ (%)
199	07/18/91	13:24	30.42	94.71	19.7	295	13.2	284	2.9	31	33%
201	07/20/91	19:02	30.42	94.81	6.1	343	2.0	295	2.9	31	67%
204	07/23/91	16:51	30.41	94.78	9.0	314	1.9	309	8.3	335	79%
205	07/24/91	06:06	30.44	94.69	13.9	310	10.7	264	7.7	11	23%
206	07/25/91	01:52	30.38	94.64	14.7	294	14.0	254	2.9	31	5%
209	07/28/91	23:58	30.40	94.74	12.5	267	19.6	8	15.2	215	0%
210	07/29/91	15:48	30.42	94.69	11.2	307	9.1	281	8.3	335	19%
211	07/30/91	22:22	30.43	94.74	8.8	295	3.1	246	8.3	335	64%
<b>222</b>	08/10/91	20:21	33.97	92.18	13.5	348	4.2	319	7.7	13	69%
239	08/27/91	05:14	34.37	91.84	33.4	314	26.3	314	3.1	35	21%
242	08/30/91	14:32	34.60	97.56	24.5	64	27.7	78	7.3	110	0%
245	09/02/91	11:05	37.77	95.57	48.6	11	43.7	12	7.5	110	10%
251	09/08/91	23:54	36.71	98.66	12.2	21	11.4	56	8.1	337	6%
252	09/09/91	21:54	28.69	94.94	15.4	206	28.9	183	13.0	344	0%
255	09/12/91	23:06	29.68	95.62	11.4	302	1.1	22	9.0	254	90%
263	09/20/91	11:16	36.24	100.16	20.8	20	16.2	27	7.7	166	22%
270a	09/27/91	07:39	34.77	99.02	19.3	34	17.0	70	8.2	336	12%
270b	09/27/91	11:56	29.82	90.36	58.0	187	27.7	183	8.3	335	52%
270c	09/27/91	23:31	30.91	95.63	266.6	129	273.7	129	3.0	33	0%
283	10/10/91	00:39	34.50	89.60	23.8	294	8.1	306	3.1	35	66%
323	11/19/91	01:04	32.49	93.82	43.1	359	23.5	11	25.4	152	45%
325	11/21/91	13:37	34.02	90.14	28.7	327	28.7	327	10.1	42	0%
328	11/24/91	07:35	34.04	88.94	11.8	19	15.2	66	7.3	110	0%
329	11/25/91	10:08	34.02	88.89	10.5	35	11.6	72	4.2	233	0%
330a	11/26/91	15:31	33.99	88.92	19.7	10	21.2	24	8.2	204	0%
<b>330b</b>	11/26/91	21:16	34.14	94.27	5.2	54	5.2	54	4.2	307	0%
<b>336</b>	12/02/91	19:45	32.10	94.56	10.6	247	14.9	198	15.5	299	0%
343	12/09/91	05:56	33.59	94.00	15.6	246	12.0	200	22.6	4	23%
348	12/14/91	08:20	34.04	88.83	15.5	349	10.7	345	3.0	35	31%
349	12/15/91	15:59	30.14	93.88	23.2	329	16.4	335	7.0	111	29%
351	12/17/91	20:27	34.04	88.83	15.9	318	12.6	302	4.2	307	20%
357a	12/23/91	01:58	34.05	88.84	25.1	346	14.4	356	4.2	307	43%
357b	12/23/91	02:14	34.01	88.86	18.9	323	8.1	309	8.2	336	57%
358	12/24/91	21:27	29.98	92.41	20.8	234	20.8	215	2.9	31	0%
360	12/26/91	13:24	30.92	99.50	13.8	306	11.3	260	2.9	148	18%
365	12/31/91	21:14	30.91	99.67	24.3	8	14.4	13	7.1	111	41%
2	01/02/92	02:35	34.09	88.76	29.0	329	17.8	326	3.0	35	39%
8	01/08/92	17:41	30.00	92.32	19.9	228	28.8	189	11.4	311	0%
<b>23</b>	01/23/92	10:26	34.52	93.21	2.1	256	6.3	151	3.1	35	0%
<b>34</b>	02/03/92	15:44	34.60	93.23	19.5	347	9.0	3	8.2	336	54%
37	02/06/92	03:35	29.71	95.66	19.4	347	13.8	2	2.9	150	28%
40	02/09/92	12:44	29.74	95.68	19.5	339	10.8	320	7.0	69	45%
76	03/16/92	01:18	34.50	86.33	24.6	358	21.7	25	4.1	307	12%
90	03/30/92	18:29	32.53	93.82	657.0	332	637.0	331	20.9	33	3%
104	04/13/92	03:47	31.75	88.22	20.7	226	26.4	202	3.0	33	0%
109	04/18/92	18:19	36.07	92.76	16.8	106	11.0	89	7.4	110	34%
137	05/16/92	20:19	36.31	100.27	25.4	35	25.2	51	4.0	232	1%
139	05/18/92	19:55	34.79	86.53	11.3	148	23.3	114	4.1	307	0%
143	05/22/92	05:47	30.89	99.70	26.5	0	8.3	38	12.6	7	69%
155	06/03/92	02:42	33.96	88.94	20.0	315	10.0	336	7.2	110	50%

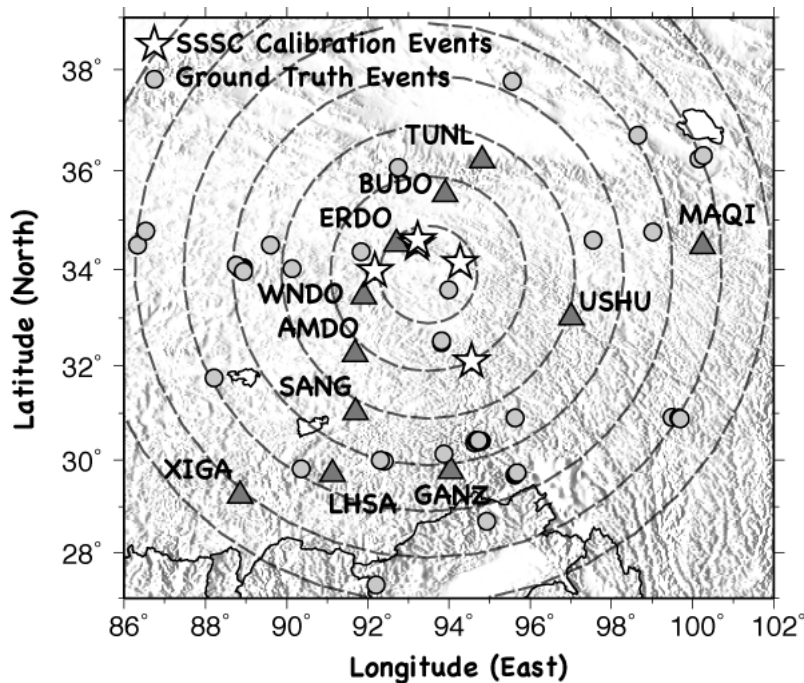


Figure 1. Location map of the 5 station correction calibration events and other GT5-GT10 events used in this study. The distance rings are at 1 degree increments centered on the centroid location of the 5 calibration events.

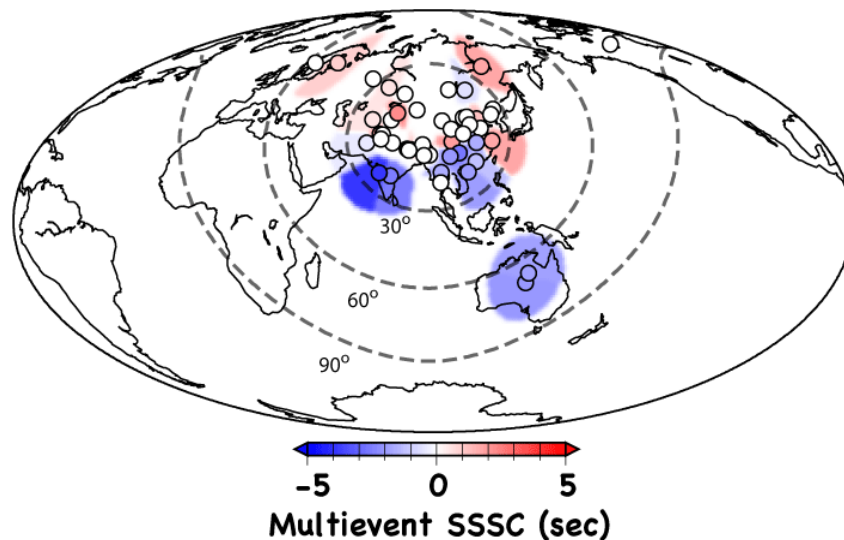


Figure 2. Global P-wave travel-time correction surface constructed using station residuals from 5 of the best-located seismic events within central Tibetan Plateau region from the GT catalog. The average station residuals from 2 or more events were used only if the value was below 1 standard deviation. The surface was constructed using the nearest neighbor algorithm. The 3 distance rings are centered at the centroid of the 5 GT event locations (33.87N, 93.49E) and are spaced in 30-degree increments.

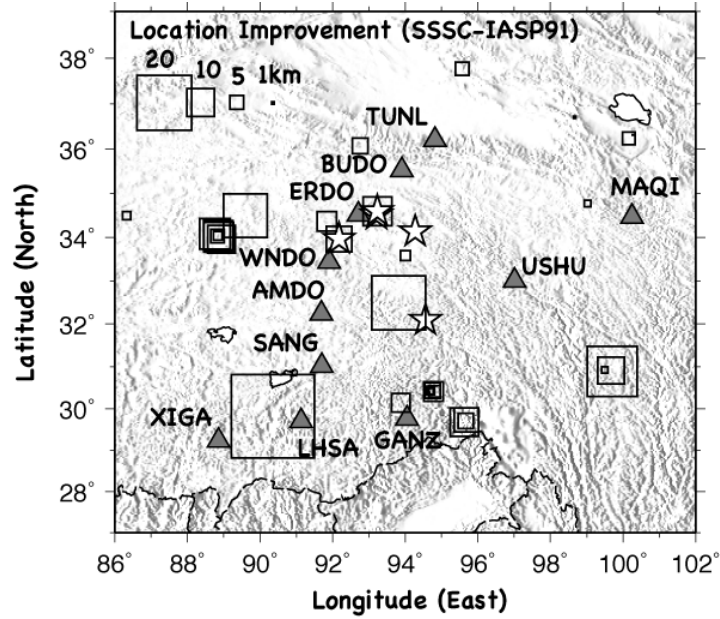


Figure 3. Location improvement in km, that is the difference between the mislocations with and without the P-wave travel-time corrections relative to the iasp91 model.

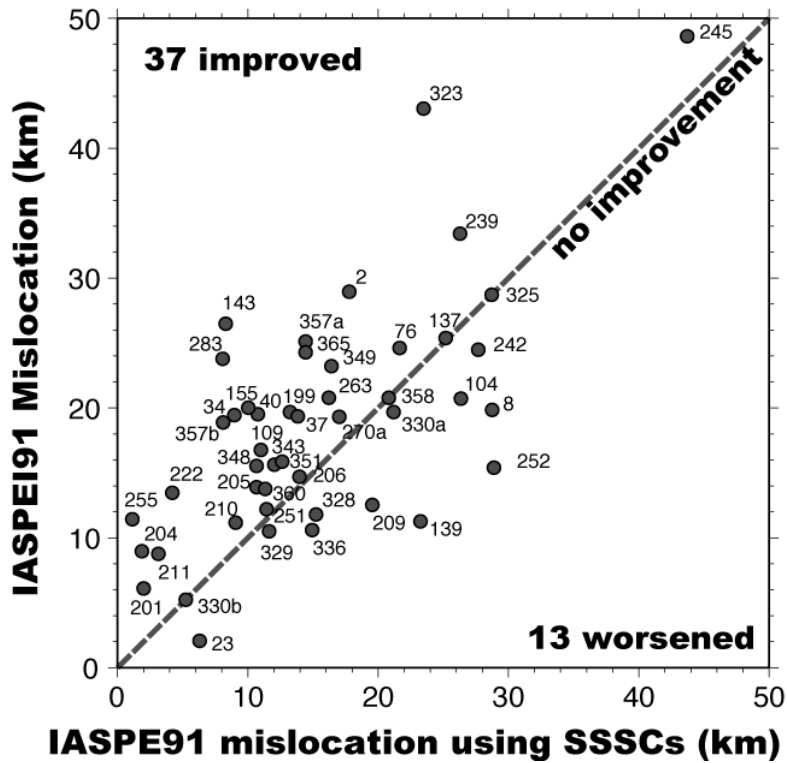


Figure 4. Mislocation plot for the 50 GT5-10 events with and without the multievent P-wave travel-time corrections. A total of 37 events improved in location while 13 events worsened in location relative to the GT catalog location.